Seismic capacity of adobe dwellings

N. Tarque
Istituto Universitario di Studi Superiori - ROSE School, Pavia, Italy
Civil Engineering Department, Catholic University of Peru, Peru

H. Crowley
European Centre for Training and Research in Earthquake Engineering, Italy

R. Pinho
Structural Mechanics Department, University of Pavia, Italy

H. Varum
Civil Engineering Department, University of Aveiro, Portugal

ABSTRACT
In this paper the seismic capacity of adobe dwellings, in-plane and out-of-plane, is analyzed in terms of the displacement capacity and the period of vibration. For the former, cyclic and dynamic tests carried out at the Catholic University of Peru (PUCP) has been analyzed to obtain limit states (LS) for adobe walls and damping values for each LS. The period of vibration obtained from the experimental test results were compared with the results of elastic numerical analysis, where different configurations of adobe buildings were simulated. Then, an expression to compute the elastic period of vibration of adobe dwellings was obtained in function of the walls height. For the out-of-plane behaviour the displacement capacity is obtained from a linearized displacement-based approach, which estimates the maximum displacement that an adobe wall can support without collapsing. The period of vibration is obtained based on the collapse mechanism selected for each wall, which is a function of the wall geometrical properties and the boundary conditions.

Keywords: adobe dwellings, displacement capacity, period of vibration

1. INTRODUCTION

When a strong earthquake occurs in areas where earthen building is common, a widespread damage to housing and significant loss of life due to the collapse of these constructions can happens. Typically, adobe houses do not have rigid diaphragms that impose similar displacement to all the walls, when subjected to seismic demands. In this case, each wall will respond independently. Based on the analysis of a damage survey carried out after the last big earthquake in Peru, 2007, the majority of adobe dwellings collapsed because of the instability of walls loaded with perpendicular forces, especially the façade walls which were supporting even the roof (Blondet *et al*. 2008).

2. IN-PLANE CAPACITY

The principal failure pattern of adobe houses is given by the overturning of the walls, specially the façade walls. However, when adobe walls are well connected, or have some buttresses, in-plane failure can be expected. The typical crack pattern due to shear forces in the plane of walls is the X-diagonal shape (Figure 1). Regarding Webster (2008), these kinds of cracks are not particularly serious unless the relative displacement across them becomes large, which means the overturning of the small blocks of walls formed by the cracks. Associated to the in-plane behaviour, some horizontal cracks can even be produced. These last cracks are related to the sliding failure. Generally, diagonal cracks start at the zones of stress (tension) concentration, as the corners of doors and windows, and run towards the top and bottom of the wall.

The in-plane seismic capacity of the walls can be represented by a limit state displacement capacity. This displacement could be compared with the displacement demand from a response spectrum at the

limit state period of vibration to ascertain whether the limit state is exceeded or not.

2.1 Limit states and displacement capacity

From the cyclic test performed by Blondet *et al.* (2005) at the Catholic University of Peru, and based on the structural damage observed during the test, four limit states have been considered with different levels of drift (Figure 2). Until 0.052% drift the structure can be considered as elastic (LS1), which means fully operational. After that, the structure may have some cracking but is still functional until 0.1% of drift (LS2). Then the life-safety performance (LS3) is reached at 0.26% of drift and, finally, the structure is considered near collapse at 0.52% of drift. These limit states are close to the values proposed for unreinforced masonry buildings by Calvi (1999); however, it is recognized that additional laboratory tests on adobe walls are necessary to achieve more precise values.

Figure 1. Failure of walls due to in-plane forces.

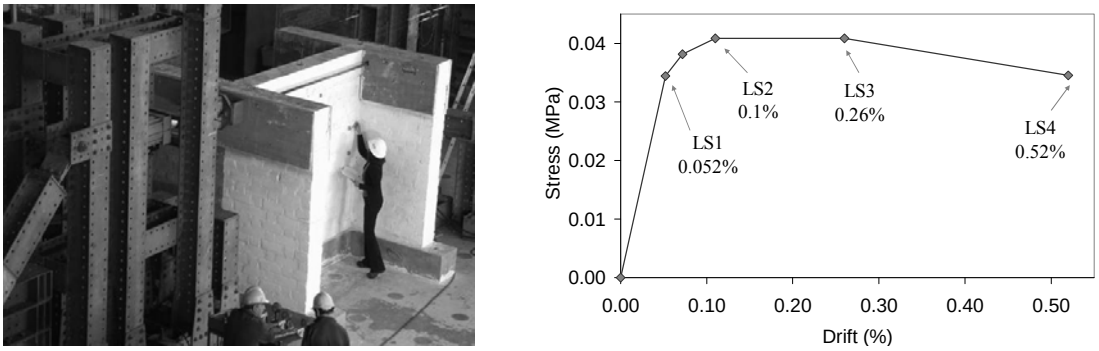

a) Cyclic test on an adobe wall b) Capacity curve

Figure 2. Experimetal test on an adobe wall (Blondet *et al.* 2005).

The maximum displacement for a given limit state (Δ_{LS}) can be represented as the summation of the yield displacement Δ_y and the plastic displacement Δ_p (Equations 2.1, 2.2 and 2.3), which are obtained from the inter-storey drift capacity of the walls at the yield and ultimate limit states (Δ_y and Δ_{LS}, respectively).

$$\Delta_y = k_1 \cdot \delta_y \cdot h_T \tag{2.1}$$

$$\Delta_p = k_2 \cdot \left(\delta_{LS} - \delta_y\right) \cdot h_{sp} \tag{2.2}$$

$$\Delta_{LS} = \Delta_y + \Delta_p \tag{2.3}$$

where h_T is the height of the storey and h_{sp} is the height of the pier.

The conversion from a multi-degree-of-freedom (MDOF) system to a SDOF system is represented by the coefficients k_1(≈ 0.80) and k_2 (≈ 0.95), which depends on the mass distribution and on the effective

height of the piers going to the inelastic range, h_{sp} (Restrepo-Velez and Magenes 2004).

2.2 Period of vibration

Estimates of the elastic period of vibration of adobe buildings were obtained from two experimental tests carried out at the Catholic University of Peru (PUCP). The first test was a displacement controlled cyclic test (push and pull test) carried out on an adobe wall by Blondet *et al.* (2005). The wall had an I-shape configuration (see Figure 2a) and it was built over a reinforced concrete foundation beam. At the top, a reinforced concrete crown beam was built to provide the gravity loading corresponding to the roof of a typical dwelling. The period of vibration in this case was estimated as 0.15s. The second test was a dynamic test performed over the unidirectional shaking table of the PUCP on a full-scale adobe module (Blondet *et al.* 2006). Here, a period of vibration of around 0.16s was obtained directly from a free vibration test.

The periods of vibration obtained from the experimental test results were compared with the results of numerical analyses performed with commercial finite element software for different configurations of adobe buildings (Tarque 2008). A reduced Young's modulus, 0.6*E*, was used for the computation of elastic vibration periods (eigen-values), considering that at the first limit state the adobe walls were already cracked due to shrinkage, changes in environmental conditions, lack of maintenance, etc. Analytical models with different heights and with different configurations were developed to study the influence of these parameters in the variation of the vibration period. The vibration periods obtained with the experimental tests and with the analytical models are plotted in Figure 3 showing the correlation between the period of vibration and the building height.

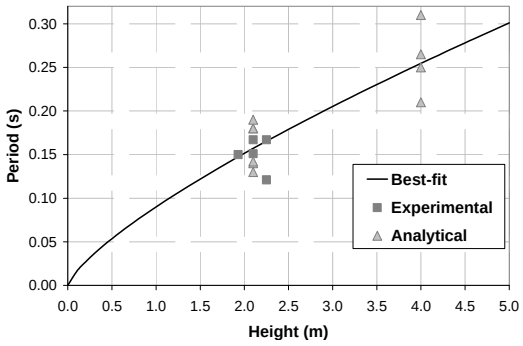

Figure 3. Vibration period versus building height.

A best-fit regression analysis was applied to the data shown in Figure 3 to obtain a vibration period versus building height, *H*, following the form $T = \alpha H^{\beta}$, which led to the following expression: $T_y = 0.09H^{3/4}$. The limit state period (T_{LSi}) can be obtained from the secant stiffness at the point of maximum deflection on an idealized bi-linear force-displacement curve (Figure 4).

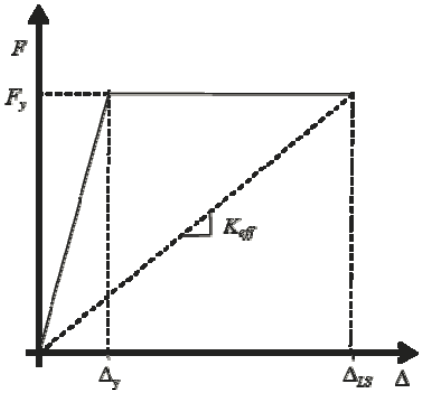

Figure 4. Elasto-plastic force displacement relation.

The effective period (T_{LSi}) of the inelastic structure can be represented as a function of the elastic period (T_y) and ductility (μ_{LSi}), as reported in Equation (2.4):

$$T_{LSi} = T_y \sqrt{\mu_{LSi}} \tag{2.4}$$

2.3 Evaluation of equivalent viscous damping in adobe walls

From the cyclic test, the equivalent viscous damping ratio for adobe walls has been calculated considering the energy absorbed in a hysteretic loop (steady-state cyclic response) due to a given displacement level (limit states). In this case, the equivalent viscous damping will be evaluated for each limit-state with Equation (2.5):

$$\xi_{hyst} = \frac{A_h}{4 \cdot \pi \cdot A_e} \tag{2.5}$$

where A_h is the area within a complete cycle of stabilized force-displacement response, and A_e is the elastic area. According to Magenes and Calvi (1997), the dissipated energy in each cycle evolves with the increase of damage and with the increase of displacement demand. Evaluating the result of adobe wall tested by Blondet *et al.* (2005), two values of equivalent damping were computed for each limit state using the first and second cycle of each hysteretic curve (Tarque 2008). The resulting values related to each of the drift limits are summarized in Table 1.

Table 1. Limit states for adobe buildings

Limit state	Description	Drift (δ_{LS})	ζ (%)	Ductility
LS1	Operational	0.052%	10	1
LS2	Functional	0.10%	10	2
LS3	Life-safety	0.26%	12	5
LS4	Near or collapsed	0.52%	16	10

3. OUT-OF-PLANE CAPACITY

The most typical failure mechanism in adobe dwellings is the out-of-plane failure (Figure 5), which is caused by a lack of connection between adobe walls. Since adobe walls have very low resistance to tension forces, the cracks will initiate in zones subjected to tension (out-of-plane flexural stresses). Usually, vertical cracks begin at the intersection of the façade with the perpendicular walls and create a physical separation between them. The façade use to overturn after a rocking behaviour. The collapse process due to out-of-plane forces is as follows: first vertical cracks appeared on the wall's corners causing the adobe blocks in that area start to break and fall; then, horizontal cracks run along the base between the intersecting walls. The wall (façade) starts to rock back and forth out-of-plane, rotating about the horizontal crack at the base till the collapse.

The displacement-based seismic analysis for out-of-plane bending of unreinforced masonry (URM) walls developed by Doherty *et al.* (2002) and Griffith *et al.* (2003) has been applied to adobe walls in the present work, since the procedure is straightforward and is based on a linearized displacement-based approach adapted for different boundary conditions (parapets and simply supported walls, as shown in Figure 6). The main goal is to predict the response of URM walls when dynamically loaded, taking into account their reserve capacity due to rocking.

Figure 5. Out-of-plane failure.

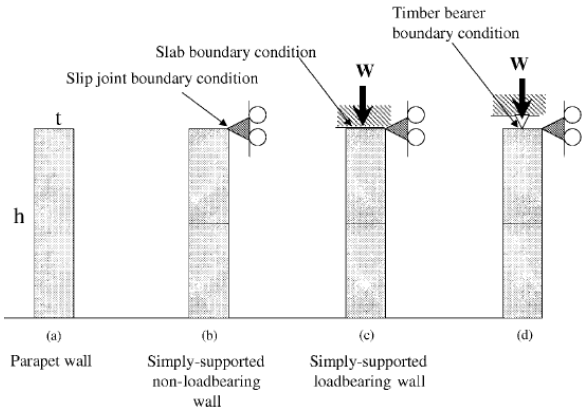

Figure 6. Unreinforced masonry walls support configurations (Doherty *et al*. 2002).

3.1 Limit states and displacement capacity

The nonlinear force-displacement response of a wall subjected to out-of-plane forces can be idealized by means of a suitable tri-linear curve defined by three displacement parameters, Δ_1, Δ_2, Δ_u and the force parameter F_0 (Doherty *et al.* 2002, Griffith *et al.* 2003, Figure 7).

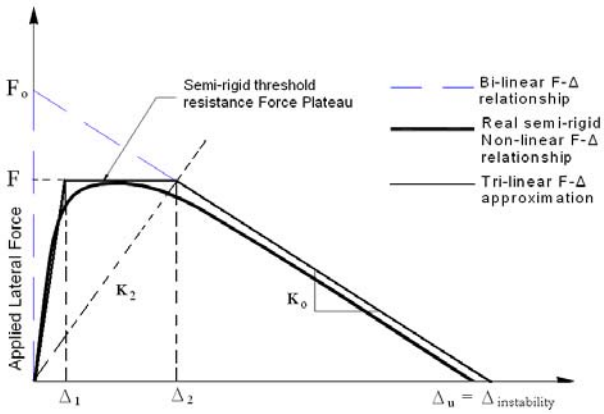

Figure 7. Trilinear idealization of the static force-displacement curve (modified from Griffith *et al*. 2003).

The displacement Δ_1 is related to the initial stiffness and Δ_2 is related to the secant stiffness K_2; Δ_u is the ultimate displacement (*i.e.* the point of static instability in the wall) and thus displacements greater than Δ_u mean that the wall will generally collapse; $F_o = \lambda W$ is the force at incipient rocking and is also called the "Rigid Threshold Resistance"; λ is the collapse multiplier factor and is calculated based on collapse mechanisms (see section 3.3), and W is the total weight of the wall.

Doherty *et al*. (2002) refers that from simple static equilibrium of the rigid parapets (Figure 6a) and simply supported walls, without axial load (Figure 6b) or with axial load applied at the leeward face (Figure 6c), the ultimate displacement Δ_u at the top and at the mid-height of the walls could be equal to the wall thickness, $\Delta_u = t$. However, for simply supported walls with axial load at the wall centreline (Figure 6d) it can be assumed that $\Delta_u \approx 0.8t$ due to the timber bearer boundary conditions. The lateral static strength (F) and the ultimate displacement (Δ_u) are not affected by uncertainties in properties such as the elasticity modulus, but instead the geometry, boundary conditions and applied vertical forces are the essential parameters (Griffith *et al.* 2003). The displacements Δ_1 and Δ_2 can be related to the material properties and the state of degradation of the mortar at the pivot points as a proportion of Δ_u (see Table 2), as proposed by Griffith *et al.* (2003).

Table 2. Displacement ratios for the tri-linear model (Griffith *et al.* 2003)

State of degradation at cracked joint	$\rho_1 = \Delta_1 / \Delta_u (\%)$	$\rho_2 = \Delta_2 / \Delta_u (\%)$
New	6	28
Moderate	13	40
Severe	20	50

According to the literature review, the ultimate limit state, defined as LS3, is related to the period of vibration evaluated with the secant stiffness (K_2). This capacity (displacement and period) can be directly compared to the displacement spectrum considering 5% damping for evaluation of fragility curves (Tarque 2008). The displacement demand is scaled by 1.5 for comparison with the displacement capacity (Griffith *et al.* 2005). If the capacity is less than the demand, the walls will completely overturn. The maximum displacement capacity at LS3 is set to be lower than the ultimate displacement: *i.e.* LS3 = $\varphi\Delta_u$, where φ is a factor from 0.8 to 1, to take into account degradation of existing masonry walls (Restrepo-Velez and Magenes 2004).

Knowing that adobe walls will have cracks at the base (due to rocking) and at the corners before they collapse, other intermediate limit states were established. In this work, LS1 and LS2 were assumed according to the author's experience and related to the grade of damage due to vertical cracks at corners (Tarque 2008). To compute the displacement capacity for LS1, a 3mm width horizontal crack at the base of the wall was assumed. Assuming that the wall will rotate as a rigid body at the base, a maximum displacement at the top of the wall of about 17mm was computed using 2.45m and 0.44m as the mean values of the wall height and thickness, respectively. The displacement capacity LS2 (Δ_1 in Figure 3) was computed directly from the displacement ratio ρ_1 times the mean value of Δ_u, resulting in a value of approximately 45mm (Table 3). For these limit states, the initial stiffness K_1 was considered for the evaluation of the period of vibration when the maximum displacements at the top of the wall were less than $0.5\Delta_u$ (as suggested by Griffith *et al.* 2003).

Table 3. Limit states for adobe walls subjected to out-of-plane demands

Limit state	Displacement capacity for parapets or simply supported walls	ζ (%)
LS1	$\approx$ 17mm	5
LS2	$\Delta_1 = \rho_1 \cdot \Delta_u$	5
LS3	$\Delta_{LSu} = \phi \cdot \Delta_u$	5

3.2 Period of vibration

Following the work of Griffith *et al.* (2003), the lateral static strength F can be evaluated using Equation (3.1) and the secant stiffness K_2, by Equation (3.2), where $F_o = \lambda W$ is the force necessary to trigger overturning and λ is the collapse multiplier.

$$F = F_o\left(1 - \frac{\Delta_2}{\Delta_u}\right) = \lambda W\left(1 - \frac{\Delta_2}{\Delta_u}\right) \tag{3.1}$$

$$K_2 = \frac{F}{\Delta_2} = \frac{\lambda W}{\Delta_2}\left(1 - \frac{\Delta_2}{\Delta_u}\right) \tag{3.2}$$

The secant stiffness K_2 is used to evaluate the period of vibration at the ultimate limit state. This is because it was found that the use of this stiffness is a reliable parameter for the determination of the displacement demand in the large amplitude displacement region (Griffith *et al.* 2003). The period of vibration for the ultimate limit state can be obtained from: $T = 2\pi(M/K_2)^{0.5}$ with the stiffness represented by Equation (3.2) and the total mass by W/g, see Equation (3.3).

$$T_{LSu} = 2\pi\sqrt{\frac{\Delta_{LSu}\cdot\rho_2}{\lambda\phi g\left(1-\rho_2\right)}} \tag{3.3}$$

The period of vibration used for the intermediate limit states (LS1 and LS2) has been related to the initial stiffness K_1 and is given by Equation (3.4).

$$T_{LSi} = 2\pi\sqrt{\frac{\Delta_1}{\lambda g\left(1-\rho_2\right)}} \tag{3.4}$$

3.3 Collapse multiplier λ

D'Ayala and Speranza (2003) have defined some typical and feasible collapse mechanisms for historical masonry buildings (Figure 8). These mechanisms have been identified through post earthquake damage inspections. According to the damage survey undertaken following the 2007 Pisco earthquake (in Peru), the most typical failure modes for 1-storey adobe buildings were related to the collapse mechanisms A, C and D, shown in Figure 4 (Blondet *et al.* 2008).

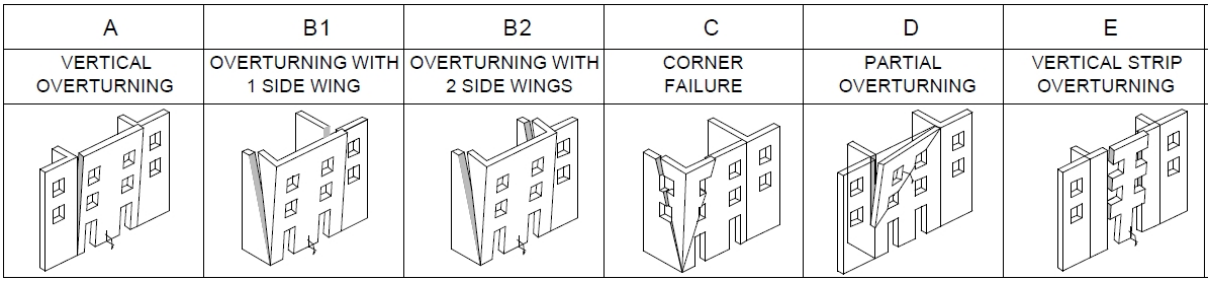

Figure 8. Typical collapse mechanisms for historical masonry buildings (D'Ayala and Speranza 2003).

D'Ayala and Speranza (2003) developed equations to calculate the associated failure load factor for each mechanism in Figure 8 (collapse multiplier, $\lambda = F/W$, that is, the ratio between the maximum lateral force for static stability over the total weight of the wall). A modification of those equations based on experimental tests was applied by Restrepo-Velez (2004) and these modified equations can be used for the evaluation of the period of vibration. Due to the extension of this paper, the equation for mechanism A is provided herein (see Equation 3.5) and the reader is referred to Restrepo-Velez (2004) for full details regarding the other mechanisms.

$$\lambda = \frac{\frac{t^2 L}{2} + \beta\cdot\Omega_{pef}\,\frac{h_s}{3}\,\mu_s\cdot s\cdot b\,\frac{(r+1)}{2} + \frac{K_r L t}{2}}{h_s\left(\frac{tL}{2} + K_r L\right)} \tag{3.5}$$

where t and L are the thickness and length of the front walls, β is the number of edge and internal perpendicular walls, Ω_{pef} is a partial efficiency factor to account for the limited effect of the friction, h_s is the height of the failing portion of the wall, μ_s is the friction coefficient, s is the staggering length (normally it is the brick half length), b is the thickness of the brick units, r is the number of courses within the failing portion (assuming courses in the rocking portion); K_r is the overburden load, in which Q_r is the load per unit length on the top of the front wall, and γ_m is the volumetric weight of masonry.

4. CONCLUSIONS

In this work the seismic capacity of adobe dwellings has been revised in terms of displacement capacity and period of vibration. The limit states for the in-plane capacity have been derived from a cyclic test and the obtained values are close to the typical values presented in the literature for unreinforced masonry buildings. The ultimate limit state for the in-plane does not mean necessarily collapse of the wall; it means that the wall has lost the capacity to resist lateral forces. In particular, shear cracks are not particularly serious unless the relative displacement across them becomes large, which means the overturning of the small blocks of walls formed by the cracks (Webster 2008). For the out-of-plane behaviour, the displacement capacity has been computed assuming no interaction with the perpendicular walls. At the beginning, adobe walls interact together during the earthquake; however, vertical cracks at the wall corner starts to appear and can disconnect the walls. The adobe blocks and the mortar can suffer disaggregation of the material at the contact zone of the rocking, so in this case the ultimate displacement Δ_u for the out-of-plane capacity should be reduced more; however, this issue should be confirmed by laboratory tests where a campaign of out-of-plane tests should be performed on adobe walls.

REFERENCES

Blondet, M., Madueño, I., Torrealva, D., Villa-García, G., and Ginocchio, F. (2005). Using industrial materials for the construction of safe adobe houses in seismic areas. *Earth Build 2005 Conference* , Sydney, Australia.

Blondet, M., Vargas, J., Torrealva, D., Tarque, N., and Velázquez, J. (2006). Seismic reinforcement of adobe houses using external polymer mesh. *First European Conference on Earthquake Engineering and Seismology ECEES*, Geneva, Switzerland.

Blondet, M., Tarque, N., and Vargas, J. (2008). Behaviour of Earthen Structures during the Pisco Earthquake. *14th World Conference on Earthquake Engineering*, Beijing, China.

Calvi, G.M. (1999). A displacement-based approach for vulnerability evaluation of classes of buildings. *Journal of Earthquake Engineering* **3**, 411-438.

D'Ayala, D., and Speranza, E. (2003). Definition of Collapse Mechanisms and Seismic Vulnerability of Historic Masonry Buildings. *Earthquake Spectra* **19**, 479–509.

Doherty, K., Griffith, M.C., Lam, N., and Wilson, J. (2002). Displacement-based seismic analysis for out-of-plane bending of unreinforced masonry wall, *Journal of Earthquake Engineering and Structural Dynamic* **31**, 833-850.

Griffith, M.C., Magenes, G.M., Melis, G., and Picchi, L. (2003). Evaluation of Out-of-Plane Stability of Unreinforced Masonry Walls Subjected to Seismic Excitation. *Journal of Earthquake Engineering* **7**, special Issue No. 1, 141-169.

Griffith, M.C., Lam, M., and Wilson, J. (2005). Displacement-based assessment of the seismic capacity of Unreinforced Masonry walls in bending. *Australian Journal of Earthquake Engineering*, Vol. 6, No. 2.

Magenes, G., and Calvi, G.M. (1997). In-plane seismic response of brick masonry walls. *Journal of Earthquake Engineering and Structural Dynamics* **26**, 1091-1112.

Restrepo-Velez L. (2004). Seismic Risk of Unreinforced Masonry Buildings, Doctoral Thesis, European School for Advanced Studies in Reduction of Seismic Risk (ROSE School). University of Pavia, Pavia, Italy.

Restrepo-Velez, L., and Magenes, G. (2004). Simplified Procedure for the Seismic Risk Assessment of Unreinforced Masonry Buildings. *13th World Conference on Earthquake Engineering*, Paper No. 2561, Vancouver, Canada.

Tarque, N. (2008). Seismic Risk Assessment of Adobe Dwellings. European School for Advanced Studies in Reduction of Seismic Risk (ROSE School), University of Pavia, Pavia, Italy. Available at October 2009 from: http://www.roseschool.it/index.php?option=com_docman&task=doc_download&gid=183&mode=view

Webster, F. (2008). Earthen Structures: Assessing Seismic Damage, Performance, and Interventions, *Terra Literature Review: An Overview of Research in Earthen Architecture Conservation*, The Getty Conservation Institute, 69-79. Available at June 2009 from http://www.getty.edu/conservation/publications/pdf_publications/terra_lit_review.pdf